Published in final edited form as:
Cancer Res. 2007 March 15; 67(6): 2729–2735. doi:10.1158/0008-5472.CAN-06-4102.

Effect of Vascular Normalization by Antiangiogenic Therapy on Interstitial Hypertension, Peritumor Edema, and Lymphatic Metastasis: Insights from a Mathematical Model

Rakesh K. Jain, **Ricky T. Tong**, and **Lance L. Munn**
E.L. Steele Lab for Tumor Biology, Department of Radiation Oncology, Massachusetts General Hospital and Harvard Medical School, Boston, Massachusetts

Abstract

Preclinical and clinical evidence shows that antiangiogenic agents can decrease tumor vessel permeability and interstitial fluid pressure (IFP) in a process of vessel "normalization." The resulting normalized vasculature has more efficient perfusion, but little is known about how tumor IFP and interstitial fluid velocity (IFV) are affected by changes in transport properties of the vessels and interstitium that are associated with antiangiogenic therapy. By using a mathematical model to simulate IFP and IFV profiles in tumors, we show here that antiangiogenic therapy can decrease IFP by decreasing the tumor size, vascular hydraulic permeability, and/or the surface area per unit tissue volume of tumor vessels. Within a certain window of antiangiogenic effects, interstitial convection within the tumor can *increase* dramatically, whereas fluid convection out of the tumor margin *decreases*. This would result in increased drug convection within the tumor and decreased convection of drugs, growth factors, or metastatic cancer cells from the tumor margin into the peritumor fluid or tissue. Decreased convection of growth factors, such as vascular endothelial growth factor-C (VEGF-C), would limit peritumor hyperplasia, and decreased VEGF-A would limit angiogenesis in sentinel lymph nodes. Both of these effects would reduce the probability of lymphatic metastasis. Finally, decreased fluid convection into the peritumor tissue would decrease peritumor edema associated with brain tumors and ascites accumulation in the peritoneal or pleural cavity, a major complication with a number of malignancies.

Introduction

Interstitial fluid pressure (IFP) is elevated in tumors in cancer patients (Table 1; ref. 1). We have previously shown that this elevated pressure is a result of the abnormal structure and function of blood and lymphatic vessels in tumors. The leaky vessels in tumors lack permselectivity and are unable to sustain the hydrostatic and oncotic pressure gradients across the vessel wall (2,3). As a result, IFP, which is close to zero in most normal tissues, is nearly as high as the microvascular pressure (MVP) in tumors (4,5). Tumor vessel leakiness is so extreme that a sudden, pharmacologically induced change in MVP results in an equivalent change in IFP, delayed by only about 10 s (6,7). This suggests there is unhindered fluid communication between the blood and interstitial spaces in tumors.

Requests for reprints: Rakesh K. Jain, Department of Radiation Oncology, Massachusetts General Hospital, 100 Blossom Street, Cox 7, Boston, MA 02114. Phone: 617−726−4083; Fax: 617−724−1819; E-mail: jain@steele.mgh.harvard.edu..
Current address for R. Tong: Stanford University School of Medicine, Stanford, CA 94305.

Note: Supplementary data for this article are available at Cancer Research Online (http://cancerres.aacrjournals.org/).

In normal tissues, lymphatic vessels drain excess fluid to maintain the IFP close to zero, but tumors do not seem to have functional lymphatic vessels. In many tumors, there are no structures that stain for lymphatic endothelial markers. In those tumors that do have structures that seem to be lymphatics via immunohistochemistry, the structures do not transport fluid or macromolecules (8−10). The lack of functional lymphatics in tumors contributes to the elevated IFP and probably results from compression of these vessels by proliferating cancer cells (11) and/or impaired lymphatic valves (12). The absence of lymphatic function in tumors is quite surprising, considering the prevalence of lymphatic metastasis from these tumors (9,13): it is difficult to reconcile the prevalence of lymphatic metastasis with the lack of intratumor conduits for cell entry. Our hypothesis is that the lymphatics in the tumor margin are adequate for lymphatic metastasis (8,9). However, whether and how the elevated IFP in tumors facilitates lymphatic metastasis remains to be elucidated.

To gain insight into the etiology and implications of elevated tumor IFP, we developed a mathematical model in 1988 to simulate fluid and macromolecular transport in tumors (14−17). The most striking prediction of this mathematical model, confirmed in 1990 experimentally (18), was that the IFP is relatively uniform throughout the tumor and decreases precipitously in the tumor margin. Because fluid convection, or bulk flow, requires pressure gradients, the model also predicted that convection would be negligible throughout the tumor but significant near the tumor margin. Prior and subsequent experimental studies were in concert with our model predictions, showing that fluid flow rates from the tumor margin calculated by our model were of the same order of magnitude as those measured in transplanted tumors in rodents (19−21) and colon carcinomas in patients (22).

We propose that in addition to creating peritumor edema and ascites, the fluid flowing from the tumor margin transports tumor-generated molecules and cells that facilitate angiogenesis, lymphangiogenesis, and metastasis (Fig. 1). Therefore, any therapeutic strategy that can lower the rate of fluid seepage from the tumor margin is likely to interfere with tumor dissemination and alleviate peritumor edema and ascites. Using our mathematical model, we show here that antiangiogenic therapy is one such strategy that can have a profound effect on tumor vessel transport properties, lymphatic metastasis, and tumor-associated edema.

Other recent, counter-intuitive findings have also prompted us to revisit our 1988 model. First, anti–vascular endothelial growth factor (anti-VEGF) or anti-VEGFR2 therapy has been shown to “normalize” tumor vessels (23,24) and to reduce IFP in a variety of tumors in mice and in rectal carcinomas in patients (refs. 25–30;Table 2), but it is unclear how these changes in IFP influence fluid convection within and out of the tumor. Second, direct and indirect anti–VEGF/VEGFR2 therapy can improve the penetration of therapeutics in tumors (26,31). This observation might be explained by better convection within tumors due to restored transvascular pressure gradients. Third, VEGF-C induces lymphatic hyperplasia in peritumor lymphatics, increasing their flow capacity and facilitating cancer cell transport to nearby lymph nodes; this process can be inhibited by an anti-VEGFR3 antibody (32). Fourth, VEGF-A over-expression in the primary tumor can induce lymph node angiogenesis and lymphangiogenesis and promote lymphatic metastasis from some tumors (33,34). Fifth, oral VEGF receptor kinase inhibitors can alleviate ascites formation in an ovarian cancer model in mice (35) and edema in patients with recurrent brain tumors (36).

Here, we show that our mathematical model can be used to integrate these seemingly diverse observations in a unified framework and to elucidate how vascular normalization by anti-VEGF therapies can (*a*) improve the convection of therapeutics in tumors, (*b*) decrease the

shedding of metastatic cells and growth factors out of tumors, and (*c*) alleviate peritumor edema and ascites formation.

Materials and Methods

Mathematical model

We employ here a mathematical model of a tumor growing as an isolated mass in a body cavity (e.g., peritoneal cavity, case I) or embedded in a host organ (case II; refs. 14,15). The model predicts how different transport properties of the vessel wall and the interstitium affect tumor IFP and interstitial fluid velocity (IFV). At each radial position, the relative IFP ($\hat{P}$) and relative IFV ($\hat{u}_i$) can be expressed as a function of a single variable, α (see Online Supplement for details). $\hat{P}$ is the interstitial pressure relative to the "effective pressure" P_e defined as $P_e = MVP - \rho(\pi_v - \pi_i)$. In tumors, $\pi_v \approx \pi_i$ so that P_e is approximately equal to MVP; therefore, $\hat{P}$ is the interstitial pressure relative to microvascular pressure. α represents the ratio of the rate of water movement across the blood vessel wall to the rate through the interstitial matrix. Mathematically, α is equal to $R\sqrt{\frac{L_p S}{KV}}$. Here, K is the tissue hydraulic conductivity (cm^2/mm Hg/s), and L_p is the vascular hydraulic permeability (cm/mm Hg/s). These variables describe the ease with which water moves through the interstitium (K) and across the vessel wall (L_p). R is the tumor radius, and S/V is the surface area of vessel wall per unit volume of tissue (cm^{-1}). The rate of fluid seeping from the tumor margin into the peritumor fluid or tissue is simply a product of the IFV at the tumor margin and the surface area of tumor (i.e., $4\pi R^2$).

These variables are expected to change with tumor growth and treatment. For example, VEGF produced by cancer and host cells in a tumor can increase the number and size of the pores in the vessel wall (37,38), which would increase L_p and, in turn, α. Conversely, anti-VEGF therapy can decrease the size of pores, vessel surface area, and tumor radius and thus would decrease α. The model predicts that these changes in α will affect the fluid pressure and flow within, and out of, the tumor. α influences IFP and IFV in a complicated, nonintuitive way; therefore, we used our mathematical model to help understand and quantify these effects.

To use our model to predict tumor IFP and IFV, we need direct measurements or estimates of all the model variables. None of these values were available for tumors in 1988 when this mathematical model was originally developed (14,15). Fortunately, in the intervening years, we and others have been able to experimentally determine most of the necessary variables in tumor and normal tissue. For example, we recently measured IFP, MVP, and intravascular and extravascular oncotic pressures in both the untreated and anti-VEGFR2 antibody–treated murine mammary carcinoma MCaIV transplanted in mice (26). In what follows, we estimate the remaining variables before and after vascular normalization of a given tumor. Then we calculate IFP and IFV profiles (see the Online Supplement for details of the calculations) and compare the calculated IFP with the measured values of IFP (Table 2). We then use our validated model to calculate fluid loss from the tumor periphery before and after antiangiogenic therapy for different sets of model variables. The model results help to reconcile contradictory data in the literature on IFP and lymphatic metastasis in animal and human tumors and show how vascular normalization can alleviate per-tumor edema and ascites formation.

Estimation of L_p and K

Vascular hydraulic permeability has been measured in various normal tissues in a variety of animals (3). For capillaries in skeletal muscle in rats, L_p was calculated to be 3.6×10^{-8} cm/s/mm Hg (39). We used this value for normal tissue.

For tumors, we measured a capillary filtration coefficient (i.e., L_pS/V) of ~2.7 cm^3/min/100 g/mm Hg (21). Assuming $S/V = 250$ cm^2/cm^3 (40), this translates to a hydraulic permeability of 1.86×10^{-6} cm/s/mm Hg. To estimate how L_p changes with antiangiogenic treatment, we use data from experiments in which we measured hydraulic permeability with and without VEGF treatment. We found that the addition of VEGF causes a 5-fold increase in L_p in monolayers of endothelial cells (41). This agrees well with values measured in various animal models. For example, Pocock et al. (42) found that VEGF induced a 3.8-fold increase in L_p in frog mesentery, and Bates and Curry (43) found a 7.8-fold increase in a similar system.

Therefore, we assume a 5-fold decrease in L_p when tumors are treated with an anti-VEGFR2 antibody. Thus, L_p of normalized vessels was estimated to be 3.7×10^{-7} cm/mm Hg/s. This 5-fold decrease is likely an underestimate considering that both perivascular cell and basement membrane coverage increase in MCaIV tumors during normalization (26). These processes, absent in the *in vitro* experiments, would be expected to further fortify the endothelial barrier.

For transport through the interstitium, hydraulic conductivity values (K) vary widely depending on the tissue type. For example, lung is extremely conductive, with K of ~500 cm^2/s/mm Hg, whereas cartilage has low conductivity, in the range of $K = 0.01$ to 0.1 cm^2/s/mm Hg. Mesentery and skin fall in between these extremes, with values in the range 10 to 100 cm^2/s/mm Hg (2). For the purpose of this analysis, we assume that normal tissue hydraulic conductivity will not be too different from the tumor embedded within it. In other words, the tumor originates from the host cells in which it resides; thus, as a first approximation, K may be the same for the tumor and normal tissue. We have measured K for a number of tumors and have used a representative value of 2.5×10^{-7} cm^2/s/mm Hg for MCaIV tumors (44). How the hydraulic permeability of the interstitium changes with antiangiogenic treatment is not known; thus, we assume K to be the same before and after normalization.

Estimation of S/V

S/V was calculated from intravital images of tumor vasculature (40,45). This variable showed a large amount of heterogeneity across tumor types as well as within individual tumors. The values generally fall in the range of 50 to 250 cm^{-1} for normal tumor and normalized tumor vasculature; thus, in the analysis, we consider the entire range. Regardless, as shown in multiple tumor models, antiangiogenic therapy will lower S/V compared with pretreatment levels.

Estimation of oncotic pressure contribution

The oncotic pressure contribution, which counters the hydrostatic pressure difference across the vessel wall in normal tissue, is given by $\sigma(\pi_v - \pi_i)$. The oncotic pressure coefficient σ is determined by the size of the largest pores in the vessel wall. The larger the pore size, the less selective the vessel wall will be, leading to a smaller value of σ. Decreases in pore size by antiangiogenic therapy might cause induction of permselectivity (increased σ) and establishment of an oncotic pressure difference inside versus outside the vessels. This would lower IFP and fluid convection throughout the tumors. As shown next, our analysis

suggests, however, that σ ($\pi_v - \pi_i$) is very small, even after antiangiogenic therapy; thus, oncotic pressure does not significantly influence water convection across tumor vessels.

In normal tissue, the value of σ for albumin varies between 0 for the liver (with a high vascular permeability) and 1 for the impermeable brain vessels, with lung falling in the middle of the range with a σ of 0.5 (3). In our simulations, we used σ of 0.91 for normal tissue, measured for albumin in s.c. tissue (see Table 3 and Supplementary Table S2). Because there are no measurements of σ for tumors, we estimated it using a spherical solute/cylindrical pore model (46,47). In this model, albumin was modeled as a solid sphere, and the vascular wall was assumed to have cylindrical pores. σ can be estimated as $\sigma = [1 - (1 - \lambda)^2]^2$, where $\lambda = r_s$ (solute radius)/r_o (pore radius). Bovine serum albumin is reported to have a hydrodynamic radius of around 3.5 nm (2,3). Using a functional assay, the maximum diameter of vascular pores in MCaIV tumors implanted in the dorsal skinfold chamber was found to be between 1.2 and 2 μm (37). Analysis of scanning electron microscopy measurements in the same tumors gave similar results, with intercellular openings of 1.7 μm in diameter and transcellular holes of 0.6 μm in diameter (38). Thus, for this analysis, we assumed the pore diameter to be 1.5 μm. Based on the solute and pore radii, the calculated σ was 8.7×10^{-5}, a value consistent with the extremely leaky vessels in the MCaIV tumor.

To estimate the value of σ in normalized vessels, we used the pore size measured after hormone withdrawal from a hormone-dependent tumor. Hormone withdrawal from a hormone-dependent Shionogi mammary tumor leads to a decrease in VEGF level, similar to VEGF blockade by an anti-VEGF antibody, and a decrease in maximum pore size to about one fifth of its baseline value (37,48). Thus, we estimated the pore size of normalized blood vessels to be 300 nm (one fifth of the baseline value); in this case, the calculated σ was still quite low (i.e., 2.1×10^{-3}). Even a 20-fold decrease in pore size would only increase σ to 0.03.

Recently we measured MVP, π_v, and π_i in MCaIV tumors before and after anti-VEGFR2 therapy. In this study, MVP and π_v did not change significantly (pretreatment: MVP = 5.5 mm Hg, π_v = 19.8; posttreatment: MVP = 5.3 mm Hg, π_v = 19.2 mm Hg), and there was only a slight decrease in π_i (pretreatment: π_i = 17.3; posttreatment: π_i = 15.1 mm Hg; ref. 26). Thus, the oncotic pressure difference across the vessel wall is small in tumors (~2 mm Hg) and is not greatly affected by VEGF blockade, at least in this limited study. Thus, given the small values for σ and oncotic pressure gradients, oncotic pressure–induced fluid flux across the vascular wall is negligible in this tumor. Table 3 summarizes the variable values used in our model simulations, and Supplementary Table S2 gives the literature references used to estimate these values.

Results and Discussion

Effect of vascular normalization on IFP profiles

Our lab and others' have shown that antiangiogenic therapy can lower the IFP in transplanted and spontaneous tumors (Table 2), without lowering the MVP or altering lymphatic function. However, there are no measurements to date of the changes in the spatial profile of IFP in tumors after antiangiogenic therapy. Previously, we showed that our model can predict the IFP profiles in untreated tumors (18); we now extend it to the analysis of tumors treated with antiangiogenic therapy.

To compare our calculations with the published data of Tong et al. (26), we assume variable values (such as tumor radius) consistent with that study (Table 3). Using Eqs. 8 to 13 in the Online Supplement, we calculated the IFP (Fig. 2*A* and *C*) and IFV (Fig. 2*B* and *D*) profiles for cases I and II using various values of α. The striking result is that there is a range of α in

which IFP and IFV are extremely sensitive. For example, changing α from 1 to 10 raises relative IFP in the center of the tumor from <0.2 to 1. Further increases in α do not affect IFP except near the margin. Untreated tumors are expected to have α values in the range of 7 to 17 (Table 3). As shown in Fig. 2*A* and *C*, these values lead to saturation of relative IFP that extends almost to the tumor margin, with MVP equal to IFP except in a thin shell near the boundary. This is similar to the results from our previous studies of untreated tumors (18). Antiangiogenic therapy lowers both L_p and *S/V*, resulting in α values in the range of 3.5 to 8 (Table 3). Interestingly, this is the range in which IFP decreases dramatically with decreases in α, producing significant IFP gradients and convection within the tumor (Fig. 2*B* and *D*; e.g., α = 5, *green line*).

The most important message from these simulations is that the mechanism of IFP reduction in tumors by vascular normalization depends on the baseline transport properties of the tumor. Moving α from 50 to 10 will have little effect on IFP, but moving from 10 to 1 will have dramatic consequences. This is further elucidated in Fig. 3*A* and *C*, which shows the relationship between the relative IFP at the center of the tumor, where IFP is maximum, and α. For α greater than ~6, the value of relative IFP levels off inside the tumor, becoming insensitive to changes in α. This is because the MVP is balanced by the IFP and a small oncotic pressure difference, and there is nearly zero fluid flux across the vessel walls in most regions of the tumor. Despite a 25-fold increase in permselectivity (σ) by anti-VEGF therapy, the decrease in IFP is small (<1 mm Hg). The fluid that does flow out of the tumor comes from the vessels near the periphery (Fig. 1).

For tumors that have α < 6, changes in α have a significant effect on IFP. In these tumors, α (and IFP) can be lowered by decreasing the hydraulic permeability of tumor vessels (L_p), surface area of tumor vessels (*S/V*), or tumor radius (*R*) or by increasing the hydraulic conductivity of the tumor matrix (*K*). Indeed, antiangiogenic therapies have been shown to lower three of these variables in tumors (L_p, *S/V*, and *R*). Whether these therapies can also increase the hydraulic permeability (*K*) of tumors is not known. In any case, these simulations indicate that the magnitude of IFP change in a given tumor depends on the range of α values achievable.

Effect of vascular normalization on IFV

Unlike IFP, there are no reported measurements of IFV profiles in tumors. In cases in which experimental data are difficult to obtain, a mathematical model can provide useful insight, as long as it can be validated independently. We previously validated our model by comparing the rate of fluid loss from the surface of a tumor with that predicted by the model (14,15). In subsequent work, the model predictions were consistent with measurements of fluid loss from human colon carcinomas surgically excised from patients (22). Thus, the model seems to provide reasonable predictions of IFV.

With this as a basis, we calculated the IFV profiles with various values of α. As shown in Fig. 2*B*, there is a regime near α = 5 in which convection within the tumor is higher, but flow from the boundary is lower than tumors with higher α values (i.e., the lines cross). This is due to the lowering of IFP, which allows redistribution of flow: flux from vessels at the periphery decreases, and that from deeper vessels increases (Fig. 2*B* and *D*). Again, this is within the range of α that we estimate for normalized tumors. Thus, drugs injected before normalization might be washed out directly from peripheral vessels across the tumor boundary, but delivery of injected drugs after normalization would be significantly improved inside the tumor, whereas less drugs will be washed out of the tumor margin. Note that in tissue with α less than ~1, IFP will be close to 0, with hardly any gradient in the interstitium, and IFV will be correspondingly small everywhere. Thus, excessive decreases in α could hinder drug delivery.

These results have important implications for cancer prevention and treatment. Increased intratumor convection is likely to facilitate distribution and penetration of therapeutics throughout the tumor, and decreased fluid loss from the tumor surface is likely to decrease the convective loss (bulk flow) of therapeutics or growth factors (e.g., VEGF-A and VEGF-C) into the surrounding fluid/tissue. In addition to alleviating peritumor edema, measured in brain tumor patients (36), a decrease in the delivery of VEGF-A will decrease the likelihood of angiogenesis and lymphangiogenesis in the nearby tissues and lymph nodes, and a decrease in delivery of VEGF-C will attenuate hyperplasia of peritumor lymphatics. Finally, in addition to a decrease in ascites from ovarian cancer, measured in mice (35), the reduction in fluid loss from the tumor margin is likely to decrease the delivery of cancer cells into the body cavities (e.g., peritoneal or pleural cavity) or to the hyper-plastic lymphatics in the tumor margin.

In tumors with α close to 5 after antiangiogenic therapy, it is also possible that the flux of growth factors reaching the draining lymph nodes will be decreased due to less fluid flow from the boundary (Fig. 2*D*); this could also inhibit lymph node lymphangiogenesis (33). Lymph node lymphangiogenesis is thought to increase the incidence of lymph node metastasis, potentially by providing additional opportunities for cell entry into the lymphatic system. Collectively, these simulations suggest that antiangiogenic therapy and the resulting vascular normalization will improve the delivery/penetration of therapeutics in tumors, alleviate peritumor fluid accumulation, and, at the same time, decrease the shedding of cancer cells into peritumor fluid or tissue.

Relationship between IFP and lymphatic metastasis

It is tempting to assert that elevated IFP should increase lymphatic metastasis: indeed, one study in the literature supports this notion (49). On the other hand, we and others have not seen any correlation between these two variables (9,50). Our hypothesis is that it is not the IFP but the gradient of IFP in the tumor margin (which is proportional to the rate of fluid "seeping" from the tumor surface) that determines how much VEGF-A/VEGF-C/VEGF-D and how many cancer cells enter the peritumor lymphatics. In any system, flow rate is determined by pressure gradients rather than absolute pressure. We used our model to address this question by calculating the relative IFP in the tumor center (IFP_{max}) and IFV at the tumor boundary (IFV_{max}). As shown in Fig. 3*A* and *C*, we find that IFP_{max} is relatively insensitive to α for $\alpha > 6$, typical values for tumors, but it decreases monotonically for $\alpha < 6$. IFV_{max} also decreases significantly as α decreases (Fig. 3*B*). As a result, the relationship between IFV_{max} and IFP_{max} is not strictly linear (Fig. 3*C* and *D*). Assuming lymphatic metastasis is proportional to IFV_{max} (32), it is likely to be independent of IFP for most tumors, where $\alpha > 6$. However, for tumors in which $\alpha < 6$, lymphatic metastasis is likely to be proportional to IFP.

In conclusion, we show here that vascular normalization can decrease tumor IFP in a number of ways: increasing tumor hydraulic conductivity (*K*) and/or by lowering vessel hydraulic permeability (L_p), surface area to volume ratio (*S/V*), or tumor size (*R*). We also show that the fluid convection into the peritumor tissue or fluid can be lowered by normalizing the structure of tumor vessels and decreasing tumor size and/or its hydraulic permeability. Thus, normalization is likely to decrease peritumor edema, a major cause of morbidity in brain tumors (36). Decrease in convective flow from the tumor margin is also likely to lower the dissemination of cancer cells to the body fluid surrounding a tumor mass, when the tumor is located in a body cavity (e.g., peritoneal cavity). If the tumor is located in host organ with lymphatics, then the decreased convective flow out of the tumor is likely to decrease dissemination of cancer cells to lymph nodes. Additionally, the decreased convective flow of growth factors at the edge of the tumor may reduce angiogenesis and lymphangiogenesis in the draining lymph nodes. Finally, the normalized vessels fortified by

pericytes will be resistant to cancer cell invasion, a prerequisite for hematogenous metastasis. It is important to point out that the vascular normalization could be brought about not only by blocking VEGF or VEGFR2 but also possibly by blocking VEGF-C or VEGFR3, as a fraction of tumor vessels are VEGFR3 positive (8). In addition, endogenous inhibitors of angiogenesis, such as thrombospondin, endostatin, and tumstatin, could also do the same (24,51).

Supplementary Material

Refer to Web version on PubMed Central for supplementary material.

Acknowledgments

Grant support: Grants P01 CA080124 and R01 CA085140 (R.K. Jain and L.L. Munn). The costs of publication of this article were defrayed in part by the payment of page charges. This article must therefore be hereby marked *advertisement* in accordance with 18 U.S.C. Section 1734 solely to indicate this fact.

We thank Drs. Yves Boucher, William Deen, Michael Dupin, Dai Fukumura, Angera Kuo, Delphine Lacorre, Johanna Lahdenranta, Satoshi Nagano, Gregory Nelson, Tim Padera, and Yannis Perentes for helpful discussions.

References

1. Jain RK. Barriers to drug delivery in solid tumors. Sci Am 1994;271:58–65. [PubMed: 8066425]
2. Jain RK. Transport of molecules in the tumor interstitium: a review. Cancer Res 1987;47:3038–50.
3. Jain RK. Transport of molecules across tumor vasculature. Cancer Metastasis Rev 1987;6:559–94. [PubMed: 3327633]
4. Boucher Y, Jain RK. Microvascular pressure is the principal driving force for interstitial hypertension in solid tumors: implications for vascular collapse. Cancer Res 1992;52:5110–4. [PubMed: 1516068]
5. Boucher Y, Leunig M, Jain RK. Tumor angiogenesis and interstitial hypertension. Cancer Res 1996;56:4264–6. [PubMed: 8797602]
6. Netti PA, Baxter LT, Boucher Y, Skalak R, Jain RK. Time-dependent behavior of interstitial fluid pressure in solid tumors: implications for drug delivery. Cancer Res 1995;55:5451–8. [PubMed: 7585615]
7. Netti PA, Hamberg LM, Babich JW, et al. Enhancement of fluid filtration across tumor vessels: implication for delivery of macromolecules. Proc Natl Acad Sci U S A 1999;96:3137–42. [PubMed: 10077650]
8. Leu AJ, Berk DA, Lymboussaki A, Alitalo K, Jain RK. Absence of functional lymphatics within a murine sarcoma: a molecular and functional evaluation. Cancer Res 2000;60:4324–7. [PubMed: 10969769]
9. Padera TP, Kadambi A, di Tomaso E, et al. Lymphatic metastasis in the absence of functional intratumor lymphatics. Science 2002;296:1883–6. [PubMed: 11976409]
10. Jain RK, Fenton BT. Intra-tumor lymphatic vessels: a case of mistaken identity or malfunction? J Natl Cancer Inst 2002;94:417–21. [PubMed: 11904313]
11. Padera TP, Stoll BR, Tooredman JB, et al. Pathology: cancer cells compress intratumour vessels. Nature 2004;427:695. [PubMed: 14973470]
12. Isaka N, Padera TP, Hagendoorn J, Fukumura D, Jain RK. Peritumor lymphatics induced by vascular endothelial growth factor-C exhibit abnormal function. Cancer Res 2004;64:4400–4. [PubMed: 15231646]
13. Nathanson S. Insights into the mechanisms of lymph node metastasis. Cancer 2003;98:413–23. [PubMed: 12872364]
14. Jain RK, Baxter LT. Mechanisms of heterogeneous distribution of monoclonal antibodies and other macromolecules in tumors: significance of elevated interstitial pressure. Cancer Res 1988;48:7022–32. [PubMed: 3191477]

15. Baxter LT, Jain RK. Transport of fluid and macromolecules in tumors. I. Role of interstitial pressure and convection. Microvasc Res 1989;37:77–104. [PubMed: 2646512]
16. Baxter LT, Jain RK. Transport of fluid and macromolecules in tumors. II. Role of heterogeneous perfusion and lymphatics. Microvasc Res 1990;40:246–63. [PubMed: 2250603]
17. Baxter LT, Jain RK. Transport of fluid and macromolecules in tumors. III. Role of binding and metabolism. Microvasc Res 1991;41:5–23. [PubMed: 2051954]
18. Boucher Y, Baxter LT, Jain RK. Interstitial pressure gradients in tissue-isolated and subcutaneous tumors: implications for therapy. Cancer Res 1990;50:4478–84. [PubMed: 2369726]
19. Butler TP, Grantham FH, Gullino PM. Bulk transfer of fluid in the interstitial compartment of mammary tumors. Cancer Res 1975;35:3084–8. [PubMed: 1182701]
20. Sevick EM, Jain RK. Blood flow and venous pH of tissue-isolated Walker 256 carcinoma during hyperglycemia. Cancer Res 1988;48:1201–7. [PubMed: 3342400]
21. Sevick EM, Jain RK. Measurement of capillary filtration coefficient in a solid tumor. Cancer Res 1991;51:1352–5. [PubMed: 1997172]
22. Less JR, Posner MC, Skalak T, Wolmark N, Jain RK. Geometric resistance to blood flow and vascular network architecture in human colorectal carcinoma. Microcirculation 1997;4:25–33. [PubMed: 9110281]
23. Jain RK. Normalizing tumor vasculature with anti-angiogenic therapy: a new paradigm for combination therapy. Nat Med 2001;7:987–9. [PubMed: 11533692]
24. Jain RK. Normalization of tumor vasculature: an emerging concept in antiangiogenic therapy. Science 2005;307:58–62. [PubMed: 15637262]
25. Lee CG, Heijn M, di Tomaso E, et al. Anti-vascular endothelial growth factor treatment augments tumor radiation response under normoxic or hypoxic conditions. Cancer Res 2000;60:5565–70. [PubMed: 11034104]
26. Tong RT, Boucher Y, Kozin SV, et al. Vascular normalization by vascular endothelial growth factor receptor 2 blockade induces a pressure gradient across the vasculature and improves drug penetration in tumors. Cancer Res 2004;64:3731–6. [PubMed: 15172975]
27. Willett CG, Boucher Y, di Tomaso E, et al. Direct evidence that the VEGF-specific antibody bevacizumab has antivascular effects in human rectal cancer. Nat Med 2004;10:145–7. [PubMed: 14745444]
28. Huber PE, Bischof M, Jenne J, et al. Trimodal cancer treatment: beneficial effects of combined antiangio-genesis, radiation, and chemotherapy. Cancer Res 2005;65:3643–55. [PubMed: 15867359]
29. Willett CG, Boucher Y, Duda DG, et al. Surrogate markers for antiangiogenic therapy and dose-limiting toxicities for bevacizumab with radiation and chemotherapy: continued experience of a phase I trial in rectal cancer patients. J Clin Oncol 2005;23:8136–9. [PubMed: 16258121]
30. Ansiaux R, Baudelet C, Jordan BF, et al. Thalidomide radiosensitizes tumors through early changes in the tumor microenvironment. Clin Cancer Res 2005;11:743–50. [PubMed: 15701864]
31. Wildiers H, Guetens G, De Boeck G, et al. Effect of antivascular endothelial growth factor treatment on the intratumoral uptake of CPT-11. Br J Cancer 2003;88:1979–86. [PubMed: 12799646]
32. Hoshida T, Isaka N, Hagendoorn J, et al. Imaging steps of lymphatic metastasis reveals that vascular endothelial growth factor-C increases metastasis by increasing delivery of cancer cells to lymph nodes: therapeutic implications. Cancer Res 2006;66:8065–75. [PubMed: 16912183]
33. Hirakawa S, Kodama S, Kunstfeld R, et al. VEGF-A induces tumor and sentinel lymph node lymphangio-genesis and promotes lymphatic metastasis. J Exp Med 2005;201:1089–99. [PubMed: 15809353]
34. Qian CN, Berghuis B, Tsarfaty G, et al. Preparing the “soil”: the primary tumor induces vasculature reorganization in the sentinel lymph node before the arrival of metastatic cancer cells. Cancer Res 2006;66:10365–76. [PubMed: 17062557]
35. Xu L, Yoneda J, Herrera C, et al. Inhibition of malignant ascites and growth of human ovarian carcinoma by oral administration of a potent inhibitor of the vascular endothelial growth factor receptor tyrosine kinases. Int J Oncol 2000;16:445–54. [PubMed: 10675474]

36. Batchelor T, Sorensen G, di Tomaso E, et al. AZD2171, a pan-VEGF receptor tyrosine kinase inhibitor, normalizes tumor vasculature and alleviates edema in glioblastoma patients. Cancer Cell 2007;11:83–95. [PubMed: 17222792]
37. Hobbs SK, Monsky WL, Yuan F, et al. Regulation of transport pathways in tumor vessels: role of tumor type and microenvironment. Proc Natl Acad Sci U S A 1998;95:4607–12. [PubMed: 9539785]
38. Hashizume H, Baluk P, Morikawa S, et al. Openings between defective endothelial cells explain tumor vessel leakiness. Am J Pathol 2000;156:1363–80. [PubMed: 10751361]
39. Rippe B, Haraldsson B. Capillary permeability in rat hindquarters as determined by estimations of capillary reflection coefficients. Acta Physiol Scand 1986;127:289–303. [PubMed: 3751629]
40. Tyrrell JA, Mahadevan V, Tong RT, et al. A 2-D/3-D model-based method to quantify the complexity of microvasculature imaged by *in vivo* multiphoton microscopy. Microvasc Res 2005;70:165–78. [PubMed: 16239015]
41. Chang YS, Munn LL, Hillsley MV, et al. Effect of vascular endothelial growth factor on cultured endothelial cell monolayer transport properties. Microvasc Res 2000;59:265–77. [PubMed: 10684732]
42. Pocock TM, Foster RR, Bates DO. Evidence of a role for TRPC channels in VEGF-mediated increased vascular permeability *in vivo*. Am J Physiol Heart Circ Physiol 2003;286:H1015–26. [PubMed: 14551041]
43. Bates DO, Curry FE. Vascular endothelial growth factor increases hydraulic conductivity of isolated perfused microvessels. Am J Physiol 1996;271:H2520–8. [PubMed: 8997313]
44. Boucher Y, Brekken C, Netti PA, Baxter LT, Jain RK. Intratumoral infusion of fluid: estimation of hydraulic conductivity and implications for the delivery of therapeutic agents. Br J Cancer 1998;78:1442–8. [PubMed: 9836476]
45. Yuan F, Chen Y, Dellian M, et al. Time-dependent vascular regression and permeability changes in established human tumor xenografts induced by an anti-vascular endothelial growth factor/vascular permeability factor antibody. Proc Natl Acad Sci U S A 1996;93:14765–70. [PubMed: 8962129]
46. Anderson JL, Malone DM. Mechanism of osmotic flow in porous membranes. Biophys J 1974;14:957–82. [PubMed: 4429773]
47. Deen W. Hindered transport of large molecules in liquid-filed pores. AIChE Journal 1987;33:1409–25.
48. Jain RK, Safabakhsh N, Sckell A, et al. Endothelial cell death, angiogenesis, and microvascular function after castration in an androgen-dependent tumor: role of vascular endothelial growth factor. Proc Natl Acad Sci U S A 1998;95:10820–5. [PubMed: 9724788]
49. Rofstad EK, Tunheim SH, Mathiesen B, et al. Pulmonary and lymph node metastasis is associated with primary tumor interstitial fluid pressure in human melanoma xenografts. Cancer Res 2002;62:661–4. [PubMed: 11830516]
50. Nathanson S, Nelson L. Interstitial fluid pressure in breast cancer, benign breast conditions and breast parenchyma. Ann Surg Oncol 1994;1:333–8. [PubMed: 7850532]
51. Izumi Y, Xu L, di Tomaso E, Fukumura D, Jain RK. Tumour biology: Herceptin acts as an anti-angiogenic cocktail. Nature 2002;416:279–80. [PubMed: 11907566]
52. Tong, R. Harvard University-MIT Division of Health Sciences and Technology. Vol. PhD. MIT; Cambridge (MA): 2005. Dynamics of vascular normalization during anti-angiogenic therapy: implications for combination therapy.; p. 167

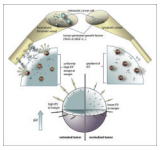

Figure 1.

The tumor is modeled as a sphere of radius *R* embedded in a body fluid (e.g., peritoneal cavity, pleural cavity) or host tissue. The interstitial fluid oozing from the tumor periphery carries therapeutics (e.g., monoclonal antibodies), growth factors (e.g., VEGF-A, VEGF-B, VEGF-C, and VEGF-D), and cells (e.g., metastatic cells) into the surrounding fluid/tissue. The result may be higher fluxes of cancer cells and growth factors from the tumor into the surrounding tissue or body fluid. The growth factors (including VEGF-A, VEGF-B, VEGF-C, and VEGF-D) can induce angiogenesis and lymphangiogenesis, and the cancer cells can contribute to metastatic dissemination via the lymphatic or blood vessels. Fluid seeping from the tumor surface can also cause edema (e.g., around brain tumors) and ascites formation (e.g., ovarian cancer). Antiangiogenic therapy can normalize the tumor vasculature, leading to lower IFP at the center, less steep IFP gradients, and lower fluid flow rates at the tumor margin, thus potentially reducing peritumor edema, ascites formation, and lymphatic metastasis. Furthermore, the normalized vessels may be more resistant to cancer cell intravasation, a prerequisite for hematogenous metastasis.

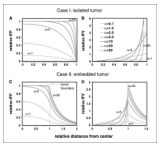

Figure 2.
Pressure and velocity distributions in an isolated tumor (*A* and *B*) and a tumor embedded in normal tissue (*C* and *D*) as a function of α. *A* and *C*, IFP. *B* and *D*, velocity profiles. α represents the ratio of rate of fluid filtration across the vessel wall and that across the interstitial matrix. Relative distance <1 represents region within the tumor, whereas >1 represents region outside of the tumor. Note that as α decreases, tumor pressure begins to decrease, and fluid velocity begins to increase in the center of tumors. On the other hand, as α decreases, the velocity at the tumor boundary decreases. For the calculations in *C* and *D*, α for normal tissue was assumed to be 2.0. Relative IFP is the actual local IFP divided by the "effective" pressure [$P_e = P_v - \sigma(\pi_v - \pi_i)$], which is approximately P_v because π_v is close to π_i, and σ is nearly zero in tumor tissue. Relative IFVis defined as the local velocity relative to an effective, or average, bulk velocity at the margin, calculated as though IFP were uniform throughout the tumor: $K(P_e)/R$ (see Online Supplement for details).

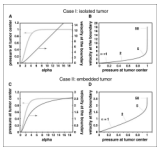

Figure 3.

Relationships between IFP near the tumor center and the fluid convection from the margin. Influence of α on the relative IFP at the center of the tumor and the fluid velocity at the tumor margin for isolated (*A*) and embedded tumor (*C*). This information is displayed again in (*B*) and (*D*), but with IFVat the boundary shown as a function of the pressure in the tumor center. Note that when *a* is greater than ~5, IFP is uniformly high throughout the tumor. Further increases in α cannot produce additional increases in IFP but do increase fluid flux from the margin. This implies that in this regime, where many tumors fall, fluid convection (and probably rates of metastasis) is insensitive to IFP at the center of the tumor.

Table 1

Interstitial pressure (mm Hg) in human tumors

Tumor type	*n*	Mean	Range
Normal skin	5	0.4	−1.0 to 3.0
Normal breast	8	0.0	−0.5 to 3.0
Head and neck carcinomas	27	19.0	1.5 to 79.0
Cervical carcinomas	127	20.5	−2.8 to 94.0
Lung carcinomas	26	9.5	1.0 to 27.0
Metastatic melanomas	26	18.0	0.0 to 60.0
Breast carcinomas	21	23.7	4.0 to 53.0
Brain tumors	28	4.6	−0.5 to 15.0
Rectal carcinoma	8	15.3	12.1 to 15.8
Colorectal liver metastasis	8	21.0	6.0 to 45.0
Lymphomas	7	4.5	1.0 to 12.5
Renal cell carcinoma	1	38.0	–

NOTE: For sources of these values, see Supplementary Table S1.

Table 2

Reduction in tumor IFP in animal and human tumors after antiangiogenic treatment

	IFP before treatment (mean ± SE, mm Hg)	IFP after treatment (mean ± SE, mm Hg)	Ref.
IFP in human tumors			
Rectal carcinoma treated with 5 mg/kg bevacizumab	15 ± 0.50 (*n* = 4)	4 ± 0.55 (*n* = 4)	(27)
Rectal carcinoma treated with 10 mg/kg bevacizumab	15.8 ± 2.0 (*n* = 5)	5.4 ± 0.85 (*n* = 5)	(29)
IFP in animal models			
Spontaneous tumor grown in C3H mice treated with DC101	11.4 ± 0.55 (*n* = 4)	4.63 ± 0.50 (*n* = 4)	(52)
MCaIV murine mammary carcinoma treated with DC101	6.13 ± 1.0 (*n* = 5)	3.10 ± 0.52 (*n* = 5)	(26)
54A human small cell lung carcinoma xenograft treated with DC101	12.03 ± 2.29 (*n* = 5)	6.2 ± 0.97 (*n* = 5)	(26)
U87 human glioblastoma xenograft treated with DC101	11.52 ± 1.89 (*n* = 5)	5.95 ± 1.06 (*n* = 5)	(26)
LS174T human colon adenocarcinoma xenograft treated with bevacizumab	13.5 ± 4.0 (*n* = 8)	3.5 ± 1.0 (*n* = 8)	(25)
U87 human glioblastoma xenograft treated with bevacizumab	12.0 ± 3.0 (*n* = 8)	3.0 ± 1.5 (*n* = 8)	(25)

Table 3

Estimated and measured variables for the model

Variable	Normal	Tumor	Normalized
R (cm)	0.4	0.4	0.4
L_p (cm/s/mm Hg)	3.6×10^{-8}	1.86×10^{-6}	3.7×10^{-7}
K (cm^2/s/mm Hg)	2.5×10^{-7}	2.5×10^{-7}	2.5×10^{-7}
S/V (cm^2/cm^3)	50−250	50−250	50−250
MVP (mm Hg)	15−25	5.5−34	≥5.3
π_v (mm Hg)	20	19.8	19.2
π_i (mm Hg)	10	17.3	15.1
σ (bovine serum albumin)	0.91	8.7×10^{-5}	2.1×10^{-3}
$\sigma(\pi_v - \pi_i)$	9.1	2.2×10^{-4}	8.6×10^{-3}
α	1.07−2.4	7.2−17	3.5−8

NOTE: For the sources of these values, see Supplementary Table S2.